Supporting Information

Ammonia Borane and Hydrazine Bis(Borane) Confined within Zirconium Bithiazole and Bipyridyl Metal-Organic Frameworks as Chemical Hydrogen Storage Materials

Giacomo Provinciali,[§,a] *Naomi Anna Consoli,*[§,b,c,d] *Rocco Caliandro,*[e] *Vincenzo Mangini,*[e] *Luisa Barba,*[f] *Cinzia Giannini,*[*,e] *Giulia Tuci,*[a] *Giuliano Giambastiani,*[c,a] *Moreno Lelli,*[*,b,c,d] *and Andrea Rossin*[*,a]

(§ These authors contributed equally)

[a] Istituto di Chimica dei Composti Organometallici (CNR-ICCOM), Via Madonna del Piano 10, Sesto Fiorentino (Firenze), 50019, Italy. E-mail: a.rossin@iccom.cnr.it

[b] Centre of Magnetic Resonance (CERM) Università di Firenze, Via Luigi Sacconi 6, Sesto Fiorentino (Firenze), 50019, Italy. E-mail: moreno.lelli@unifi.it

[c] Dipartimento di Chimica Ugo Schiff, Università di Firenze, Via della Lastruccia 3-13, Sesto Fiorentino (Firenze), 50019, Italy.

[d] Consorzio Interuniversitario Risonanze Magnetiche Metallo Proteine (CIRMMP), Via Luigi Sacconi 6, Sesto Fiorentino (Firenze), 50019, Italy.

[e] Istituto di Cristallografia (CNR-IC), via Amendola 122/o 70125 Bari (Italy).
E-mail: cinzia.giannini@cnr.it

[f] Istituto di Cristallografia (CNR-IC), Area Science PARK, ss.14 Km163.5, 34149 Basovizza (TS) (Italy).

Supporting Information

Experimental NMR parameters

Table S1. Acquisition parameters for ^{13}C CP MAS and ^{1}H-^{13}C HETCOR at 20.0 T (850 MHz) spectrometer for **Zr_PyPy**.

Experimental Parameters	^{1}H	^{13}C	
$\pi/2$ pulse (μs)	2.45	3.50	
	CP-MAS	**HETCOR**	
Acquired Nuclei	^{13}C	^{1}H	^{13}C
MAS Frequency (kHz)	20.0	20.0	
Number of scans	10240	128	
Recycle delay (s)	3.0	2.5	
Spectral width (kHz)	119.05	45.54	119.05
Acquisition time (ms)	8.6	2.2	8.6
^{1}H CP sequence	ramp 70% to 100%	ramp 70% to 100%	-
^{1}H CP power (100%) (kHz)	72.0	72.0	-
^{13}C CP sequence	constant power	-	constant power
^{13}C CP power (kHz)	50.5	-	50.5
^{1}H Decoupling sequence	SWf-TPPM[a]	SWf-TPPM[a]	-
^{1}H Decoupling power (kHz)	80.0	70.0	-
^{1}H homonuclear Power (FSLG)[b] (kHz)	-	86.0	-
Real acquired points	2048	200	2048
Window functions	Exponential (LB: 100 Hz)	Exponential (LB: 100 Hz)	Exponential (LB: 100 Hz)
Real processed points	32768	1024	4096

[a] Chandran, C. V.; Madhu, P. K.; Kurur, N. D.; Bräuniger, T. *Magn. Res. Chem.* **2008**, *46*, 943-947. [b] Lee, M.; and Goldburg, W. I. *Phys. Rev.* **1965**, *140*,1261-1271.

Supporting Information

Table S2. Acquisition parameters for ^{13}C CP MAS and ^{1}H-^{13}C HETCOR at 20.0 T (850 MHz) spectrometer for [^{15}N-AB@**Zr_PyPy**].

Experimental Parameters	^{1}H	^{13}C	
$\pi/2$ pulse (μs)	2.45	3.50	
	CP-MAS	**HETCOR**	
Acquired Nuclei	^{13}C	^{1}H	^{13}C
MAS Frequency (kHz)	20.0	20.0	
Number of scans	10240	256	
Recycle delay (s)	3.0	3.0	
Spectral width (kHz)	119.04	45.54	119.04
Acquisition time (ms)	6.8	0.5	8.6
^{1}H CP sequence	ramp 70 to 100%	ramp 70 to 100%	-
^{1}H CP power (100%) (kHz)	72.0	72.0	-
^{13}C CP sequence	constant power	-	constant power
^{13}C CP power (kHz)	50.5	-	50.5
^{1}H Decoupling sequence	SWf-TPPM[a]	SWf-TPPM[a]	
^{1}H Decoupling power (kHz)	80.0	70.0	-
^{1}H homonuclear Power (FSLG)[b] (kHz)	-	86.0	-
Real acquired points	2048	46	2048
Window functions	Exponential (LB: 90 Hz)	Exponential (LB: 100 Hz)	Exponential (LB: 100 Hz)
Real processed points	32768	1024	2048

[a] Chandran, C. V.; Madhu, P. K.; Kurur, N. D.; Bräuniger, T. *Magn. Res. Chem.* **2008**, *46*, 943-947. [b] Lee, M.; and Goldburg, W. I. *Phys. Rev.* **1965**, *140*,1261-1271.

Supporting Information

Table S3. Acquisition parameters for ^{15}N Direct Excitation (DE) and ^{1}H-^{15}N CP-MAS at 20.0 T (850 MHz) spectrometer for [^{15}N-AB@**Zr_PyPy**].

Experimental Parameters	^{15}N	
$\pi/2$ pulse (μs)	8.84	
	DE	**CP-MAS**
Acquired Nuclei	^{15}N	^{15}N
MAS Frequency (kHz)	14.0	14.0
Number of scans	8192	10240
Recycle delay (s)	5.0	4.0
Spectral width (kHz)	34.48	133.9
Acquisition time (ms)	29.7	11.4
^{1}H CP sequence	-	ramp 70 to 100%
^{1}H CP power (100%) (kHz)	-	72.0
^{15}N CP sequence	-	constant power
^{15}N CP power (kHz)	-	21.3
^{1}H Decoupling sequence	SPINAL-64[a]	SPINAL-64[a]
^{1}H Decoupling power (kHz)	80.0	80.0
Real acquired points	2048	3058
Window functions	Exponential (LB: 30 Hz)	Exponential (LB: 100 Hz)
Real processed points	8192	8192

[a] Fung, B. M.; Khitrin, A. K.; Ermolaev, K. *J. Magn. Res.* **2000**, *142*, 97–101.

Table S4. Acquisition parameters for ^{13}C CP MAS and ^{1}H-^{13}C HETCOR at 20.0 T (850 MHz) spectrometer for **Zr_TzTz**.

Experimental Parameters	^{1}H	^{13}C	
$\pi/2$ pulse (μs)	2.60	3.50	
	CP-MAS	**HETCOR**	
Acquired Nuclei	^{13}C	^{1}H	^{13}C
MAS Frequency (kHz)	20.0	20.0	
Number of scans	10240	256	
Recycle delay (s)	3.0	2.5	
Spectral width (kHz)	119.04	45.54	119.04
Acquisition time (ms)	8.6	1.4	8.6
^{1}H CP sequence	ramp 70% to 100%	ramp 70% to 100%	-
^{1}H CP power (100%) (kHz)	72.0	72.0	-
^{13}C CP sequence	constant power	-	constant power
^{13}C CP power (kHz)	50.5	-	50.5
^{1}H Decoupling sequence	SWf-TPPM[a]	SWf-TPPM[a]	-
^{1}H Decoupling power (kHz)	80.0	80.0	-
^{1}H homonuclear Power (FSLG)[b] (kHz)	-	86.0	-
Real acquired points	2048	124	2048
Window functions	Exponential (LB: 100 Hz)	Exponential (LB: 200 Hz)	Exponential (LB: 200 Hz)
Real processed points	32768	100	1024

[a] Chandran, C. V.; Madhu, P. K.; Kurur, N. D.; Bräuniger, T. *Magn. Res. Chem.* **2008**, *46*, 943-947. [b] Lee, M.; and Goldburg, W. I. *Phys. Rev.* **1965**, *140*,1261-1271.

Table S5. Acquisition parameters for ^{13}C CP MAS and ^{1}H-^{13}C HETCOR at 20.0 T (850 MHz) spectrometer for [^{15}N-AB@**Zr_TzTz**].

Experimental Parameters	^{1}H	^{13}C	
$\pi/2$ pulse (μs)	2.45	3.50	
	CP-MAS	**HETCOR**	
Acquired Nuclei	^{13}C	^{1}H	^{13}C
MAS Frequency (kHz)	20.0	20.0	
Number of scans	10240	256	
Recycle delay (s)	3.0	3.0	
Spectral width (kHz)	119.04	45.54	119.04
Acquisition time (ms)	8.6	2.2	8.6
^{1}H CP sequence	ramp 70 to 100%	ramp 70 to 100%	-
^{1}H CP power (100%) (kHz)	72.0	72.0	-
^{13}C CP sequence	constant power	-	constant power
^{13}C CP power (kHz)	50.5	-	50.5
^{1}H Decoupling sequence	SWf-TPP[a]	SWf-TPPM[a]	
^{1}H Decoupling power (kHz)	80.0	70.0	-
^{1}H homonuclear Power (FSLG)[b] (kHz)	-	86.0	-
Real acquired points	2048	200	2048
Window functions	Exponential (LB: 100 Hz)	Exponential (LB: 100 Hz)	Exponential (LB: 100 Hz)
Real processed points	16384	1024	2048

[a] Chandran, C. V.; Madhu, P. K.; Kurur, N. D.; Bräuniger, T. *Magn. Res. Chem.* **2008**, *46*, 943-947. [b] Lee, M.; Goldburg, W. I. *Phys. Rev.* **1965**, *140*,1261-1271.

Table S6. Acquisition parameters for ^{15}N Direct Excitation (DE), ^{1}H-^{15}N CP-MAS and ^{1}H-^{15}N HETCOR at 20.0 T (850 MHz) spectrometer for [^{15}N-AB@**Zr_TzTz**].

Experimental Parameters	**^{15}N**			
π/2 pulse (μs)	8.84			
	DE	**CP-MAS**	**HETCOR**	
Acquired Nuclei	^{15}N	^{15}N	^{1}H	^{15}N
MAS Frequency (kHz)	14.0	14.0	14.0	
Number of scans	8192	4096	256	
Recycle delay (s)	10.0	3.5	2.5	
Spectral width (kHz)	52.08	50.0	52.97	215.51
Acquisition time (ms)	9.8	25	0.4	23.8
^{1}H CP sequence	-	ramp 70 to 100%	ramp 70% to 100%	-
^{1}H CP power (100%) (kHz)	-	47.0	47.0	-
^{15}N CP sequence	-	constant power	-	constant power
^{15}N CP power (kHz)	-	21.3	-	21.3
^{1}H Decoupling sequence	SPINAL-64[a]	SPINAL-64[a]	SPINAL-64[a]	-
^{1}H Decoupling power (kHz)	80.0	80.0	80.0	-
^{1}H homonuclear Power (FSLG)[b] (kHz)	-	-	86.0	-
Real acquired points	1024	2500	42	1024
Window functions	Exponential (LB: 30 Hz)	Exponential (LB: 50 Hz)	Exponential (LB: 200 Hz)	Exponential (LB: 200 Hz)
Real processed points	4096	32768	1024	2048

[a] Fung, B. M.; Khitrin, A. K.; Ermolaev, K. *J. Magn. Res.* **2000**, *142*, 97–101. [b] Lee, M.; Goldburg, W. I. *Phys. Rev.* **1965**, *140*,1261-1271.

Supporting Information

Table S7. Acquisition parameters for ^{13}C CP MAS and ^{1}H-^{13}C HETCOR at 20.0 T (850 MHz) spectrometer for [^{15}N-HBB@**Zr_TzTz**].

Experimental Parameters	^{1}H	^{13}C	
$\pi/2$ pulse (μs)	3.50	3.50	
	CP-MAS	**HETCOR**	
Acquired Nuclei	^{13}C	^{1}H	^{13}C
MAS Frequency (kHz)	14.0	14.0	
Number of scans	10240	256	
Recycle delay (s)	3.0	3.0	
Spectral width (kHz)	119.04	119.04	45.54
Acquisition time (ms)	8.6	0.7	8.6
^{1}H CP sequence	ramp 70 to 100%	ramp 70 to 100%	-
^{1}H CP power (100%) (kHz)	72.0	72.0	-
^{13}C CP sequence	constant power	-	constant power
^{13}C CP power (kHz)	50.5	-	50.5
^{1}H Decoupling sequence	SPINAL-64[a]	SPINAL-64[a]	
^{1}H Decoupling power (kHz)	80.0	70.0	-
^{1}H homonuclear Power (FSLG)[b] (kHz)	-	86.0	-
Real acquired points	2048	60	2048
Window functions	Exponential (LB: 100 Hz)	Exponential (LB: 250 Hz)	Exponential (LB: 200 Hz)
Real processed points	32768	1024	2048

[a] Fung, B. M.; Khitrin, A. K.; Ermolaev, K. *J. Magn. Res.* **2000**, *142*, 97–101. [b] Lee, M.; Goldburg, W. I. *Phys. Rev.* **1965**, *140*,1261-1271.

Table S8. Acquisition parameters for ^{11}B 1D echo with decoupling for ^{11}B quantification and ^{1}H-^{11}B HETCOR at 16.4 T (701 MHz) spectrometer for [^{15}N-AB@**Zr_PyPy**].

Experimental Parameters	^{1}H	^{11}B	
π/2 pulse (μs)	2.70	8.45	
	Hahn Echo	**HETCOR**	
Acquired Nuclei	^{11}B	^{1}H	^{11}B
MAS Frequency (kHz)	12.0	12.0	
Number of scans	1024	128	
Recycle delay (s)	18	3.0	
Spectral width (kHz)	74.63	45.55	78.12
Acquisition time (ms)	3.4	0.53	4.92
^{1}H CP sequence	ramp 70 to 100%	ramp 70 to 100%	-
^{1}H CP power (100%) (kHz)	-	45.0	-
^{11}B CP sequence	constant power	-	constant power
^{11}B CP power (kHz)	-	-	16.0
^{1}H Decoupling sequence	SPINAL-64[a]	SPINAL-64[a]	
^{1}H Decoupling power (kHz)	80.0	80.0	-
^{1}H homonuclear Power (FSLG)[b] (kHz)	-	86.0	-
Real acquired points	512	48	768
Window functions	Exponential (LB: 30 Hz)	Exponential (LB: 10 Hz)	Exponential (LB: 10 Hz)
Real processed points	65536	1024	1024

[a] Fung, B. M.; Khitrin, A. K.; Ermolaev, K. *J. Magn. Res.* **2000**, *142*, 97–101. [b] Lee, M.; Goldburg, W. I. *Phys. Rev.* **1965**, *140*,1261-1271.

Table S9. Acquisition parameters for ^{11}B 1D echo with decoupling for ^{11}B quantification and ^{1}H-^{11}B HETCOR at 16.4 T (701 MHz) spectrometer for [^{15}N-AB@**Zr_TzTz**].

Experimental Parameters	^{1}H	^{11}B	
$\pi/2$ pulse (μs)	2.60	8.45	
	Hahn Echo	**HETCOR**	
Acquired Nuclei	^{11}B	^{1}H	^{11}B
MAS Frequency (kHz)	12.0	12.0	
Number of scans	1024	128	
Recycle delay (s)	18.0	4.0	
Spectral width (kHz)	74.63	45.55	78.12
Acquisition time (ms)	6.9	1.41	4.92
^{1}H CP sequence	ramp 70 to 100%	ramp 70 to 100%	-
^{1}H CP power (100%) (kHz)	-	45.0	-
^{11}B CP sequence	constant power	-	constant power
^{11}B CP power (kHz)	-	-	16.0
^{1}H Decoupling sequence	SPINAL-64[a]	SPINAL-64[a]	
^{1}H Decoupling power (kHz)	80.0	80.0	-
^{1}H homonuclear Power (FSLG)[b] (kHz)	-	86.0	-
Real acquired points	1024	60	768
Window functions	Exponential (LB: 30 Hz)	Exponential (LB: 30 Hz)	Exponential (LB: 30 Hz)
Real processed points	65536	1024	1024

[a] Fung, B. M.; Khitrin, A. K.; Ermolaev, K. *J. Magn. Res.* **2000**, *142*, 97–101. [b] Lee, M.; Goldburg, W. I. *Phys. Rev.* **1965**, *140*,1261-1271.

Table S10. Acquisition parameters for ^{11}B 1D echo with decoupling for ^{11}B quantification and ^{1}H-^{11}B HETCOR at 16.4 T (701 MHz) spectrometer for [^{15}N-HBB@**Zr_TzTz**].

Calibration	^{1}H	^{11}B	
$\pi/2$ pulse (μs)	2.70	8.45	
Experimental Parameters	**Hahn Echo**	**HETCOR**	
Nuclei	^{11}B	^{1}H	^{11}B
MAS Frequency (kHz)	12.0	12.0	
Number of scans	1024	128	
Recycle delay (s)	18.0	4.0	
Spectral width (kHz)	74.63	45.55	78.12
Acquisition time (ms)	6.9	1.32	4.92
^{1}H CP sequence	ramp 70 to 100%	ramp 70 to 100%	-
^{1}H CP power (100%) (kHz)	-	1.0	-
^{11}B CP sequence	constant power	-	constant power
^{11}B CP power (kHz)	-	-	16.0
^{1}H Decoupling sequence	SPINAL-64[a]	SPINAL-64[a]	
^{1}H Decoupling power (kHz)	80.0	80.0	-
^{1}H homonuclear Power (FSLG)[b] (kHz)	-	86.0	-
Real acquired points	1024	85	768
Window functions	Exponential (LB: 30 Hz)	Exponential (LB: 30 Hz)	Exponential (LB: 30 Hz)
Real processed points	65536	512	1024

[a] Fung, B. M.; Khitrin, A. K.; Ermolaev, K. *J. Magn. Res.* **2000**, *142*, 97–101. [b] Lee, M.; Goldburg, W. I. *Phys. Rev.* **1965**, *140*,1261-1271.

Table S11. Acquisition parameters for ^{11}B 1D echo with decoupling for ^{11}B quantification and ^{1}H-^{11}B HETCOR at 16.4 T (701 MHz) spectrometer for AB.

Experimental Parameters	^{1}H	^{11}B	
$\pi/2$ pulse (μs)	2.75	8.45	
	Hahn Echo	**HETCOR**	
Nuclei	^{11}B	^{1}H	^{11}B
MAS Frequency (kHz)	12.0	12.0	
Number of scans	4096	128	
Recycle delay (s)	18.0	4.0	
Spectral width (kHz)	74.63	1.7	9.8
Acquisition time (ms)	41.2	1.8	9.82
^{1}H CP sequence	-	ramp 70 to 100%	-
^{1}H CP power (100%) (kHz)	-	45.0	-
^{11}B CP sequence	-	-	constant power
^{11}B CP power (kHz)	-	-	16.0
^{1}H Decoupling sequence	SPINAL-64[a]	SPINAL-64[a]	
^{1}H Decoupling power (kHz)	70.0	70.0	-
^{1}H homonuclear Power (FSLG)[b] (kHz)	-	86.0	-
Real acquired points	6144	162	1536
Window functions	Exponential (LB: 30 Hz)	Exponential (LB: 200 Hz)	Exponential (LB: 200 Hz)
Real processed points	65536	1024	2048

[a] Fung, B. M.; Khitrin, A. K.; Ermolaev, K. *J. Magn. Res.* **2000**, *142*, 97–101. [b] Lee, M.; Goldburg, W. I. *Phys. Rev.* **1965**, *140*,1261-1271.

Table S12. Acquisition parameters for ^{11}B 1D echo with decoupling and ^{1}H-^{11}B HETCOR at 16.4 T (701 MHz) spectrometer for HBB.

Experimental Parameters	^{1}H	^{11}B	
π/2 pulse (μs)	2.66	2.50	
	Hahn Echo	**HETCOR**	
Nuclei	^{11}B	^{1}H	^{11}B
MAS Frequency (kHz)	14.0	14.0	
Number of scans	1024	32	
Recycle delay (s)	4.0	4.0	
Spectral width (kHz)	66.97	52.97	66.97
Acquisition time (ms)	22.9	1.4	3.7
^{1}H CP sequence	-	ramp 70 to 100%	-
^{1}H CP power (100%) (kHz)	-	80.0	-
^{11}B CP sequence	-	-	constant power
^{11}B CP power (kHz)	-	-	16.0
^{1}H Decoupling sequence	SPINAL-64[a]	SPINAL-64[a]	
^{1}H Decoupling power (kHz)	80.0	80.0	-
^{1}H homonuclear Power (FSLG)[b] (kHz)	-	86.0	-
Real acquired points	3072	150	500
Window functions	Exponential (LB: 10 Hz)	Exponential (LB: 30 Hz)	Exponential (LB: 30 Hz)
Real processed points	4096	512	4096

[a] Fung, B. M.; Khitrin, A. K.; Ermolaev, K. *J. Magn. Res.* **2000**, *142*, 97–101. [b] Lee, M.; Goldburg, W. I. *Phys. Rev.* **1965**, *140*,1261-1271.

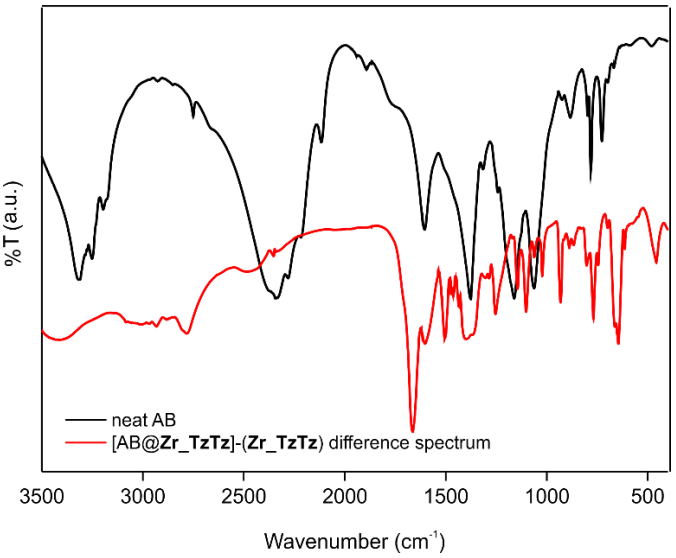

Figure S1. IR spectra (KBr pellets) in the 3500-400 cm^{-1} region of the difference spectrum {[AB@**Zr_TzTz**] – **Zr_TzTz**} and pure AB at comparison. The typical ammonia borane vibrational modes can be found in the former, confirming the hydride presence in the solid.

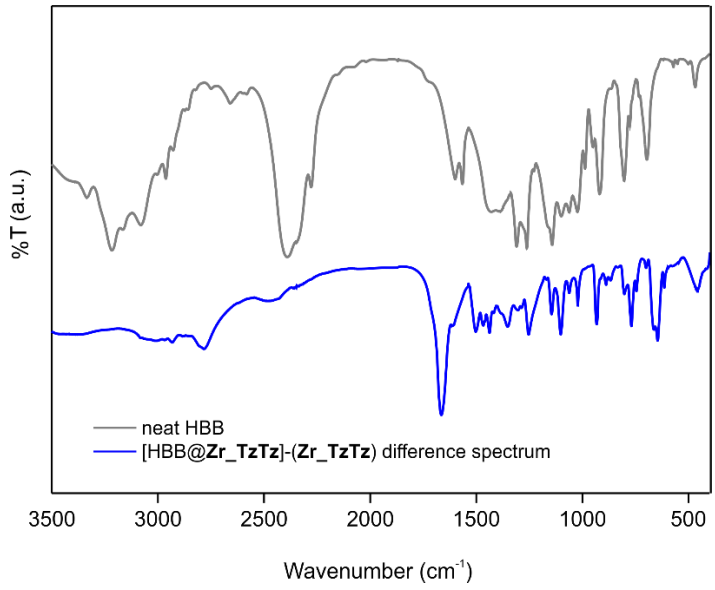

Figure S2. IR spectra (KBr pellets) in the 3500-400 cm^{-1} region of the difference spectrum {[HBB@**Zr_TzTz**] – **Zr_TzTz**} and pure HBB at comparison. The typical hydrazine bis(borane) vibrational modes can be found in the former, confirming the hydride presence in the solid.

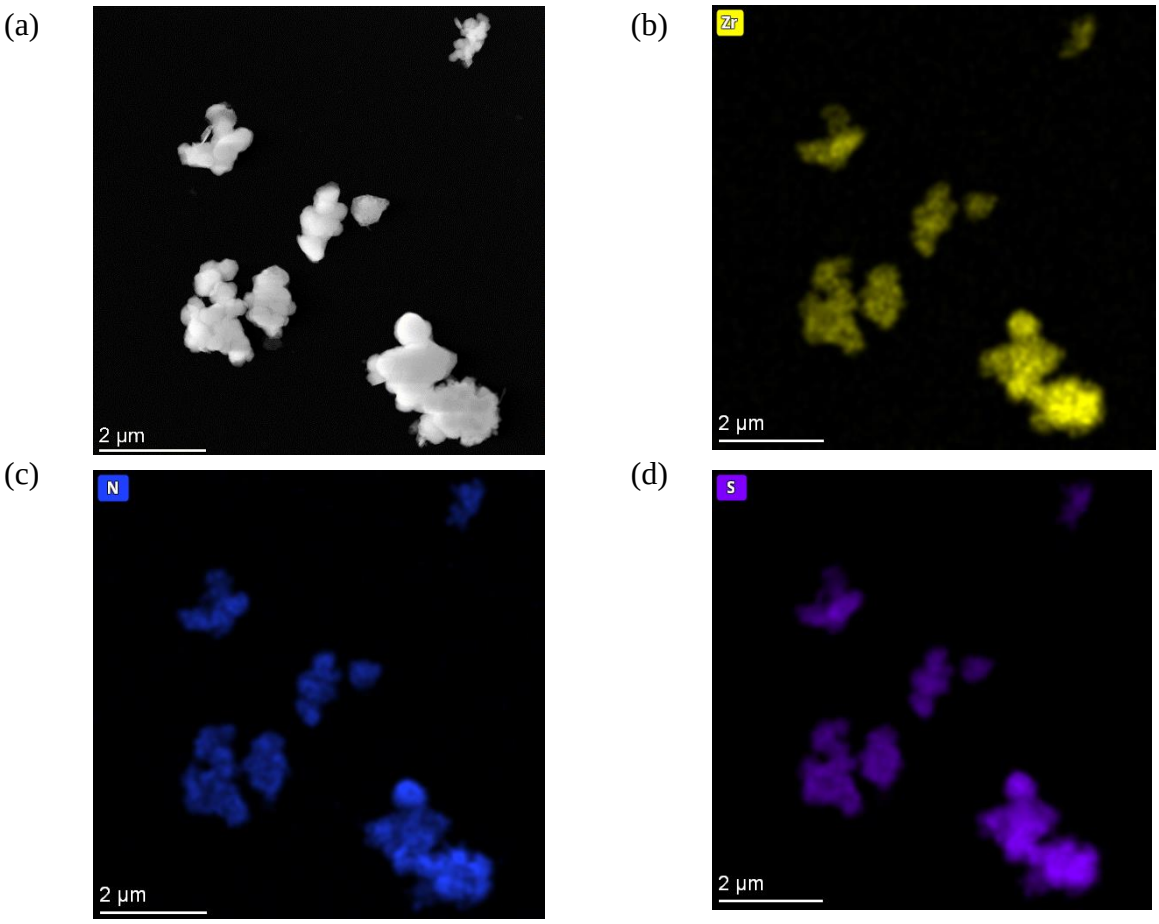

Figure S3. TEM image of [AB@**Zr_TzTz**] (a) and related zirconium (b), nitrogen (c) and sulfur (d) EDX distribution.

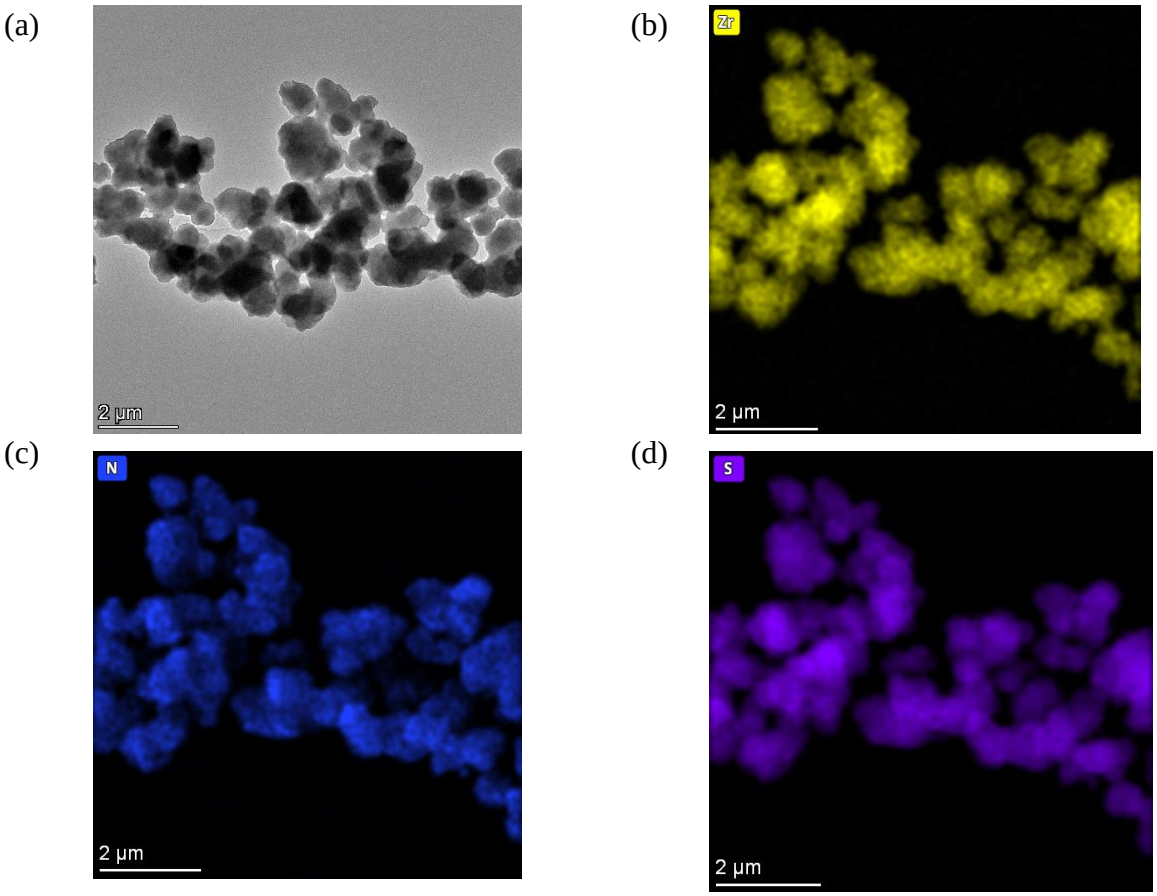

Figure S4. TEM image of [HBB@**Zr_TzTz**] (a) and related zirconium (b), nitrogen (c) and sulfur (d) EDX distribution.

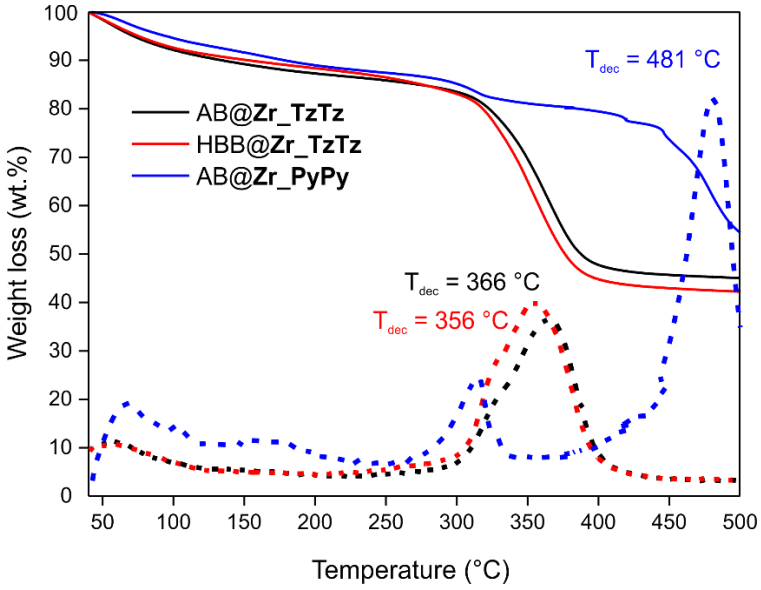

Figure S5. TG-DTG profiles of the three composites prepared in this work.

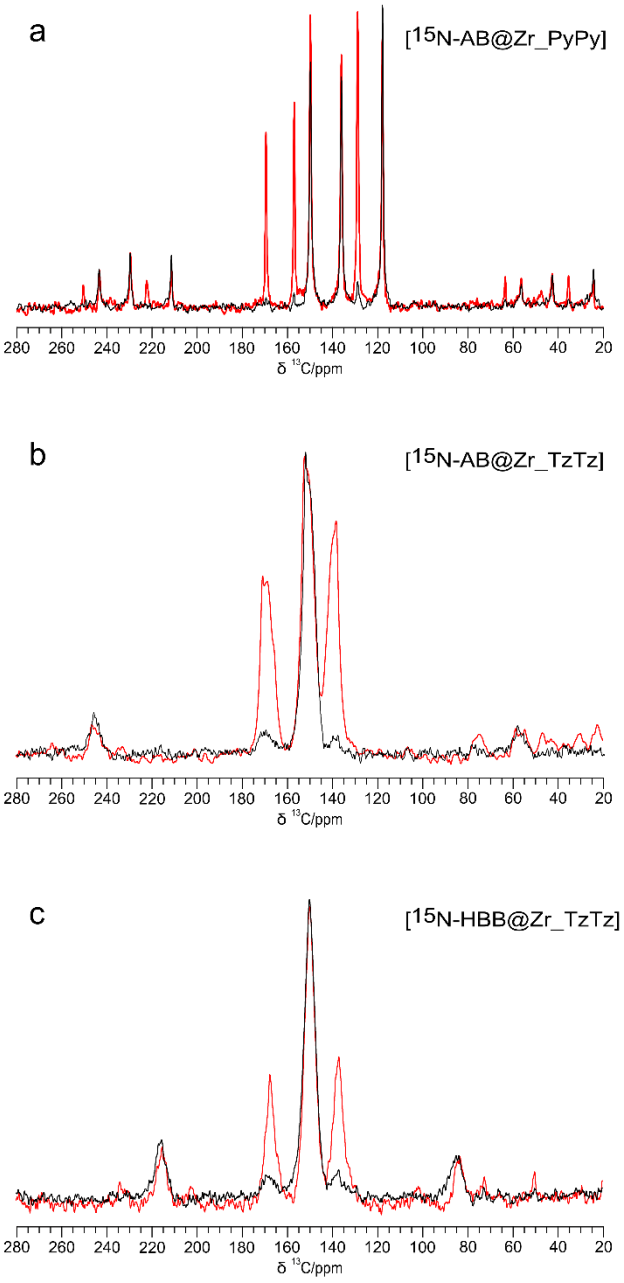

Figure S6. 1D {^{1}H}-^{13}C CP MAS spectra of [AB@**Zr_PyPy]** (a), [AB@**Zr_TzTz**] (b) and [HBB@**Zr_TzTz**] (c), acquired with two different contact times: 100 µs (black) and 1000 µs (red). The spectra are normalized to the highest peak of each compound. The spectra were acquired at 20.0 T (850 MHz of Larmor frequency) and at a temperature of –8 °C. A and B spectra were acquired at 20 kHz of MAS frequency, while C was acquired at 14.0 kHz of MAS frequency. The experimental and processing parameters are reported in Tables S3, S5 and S7.

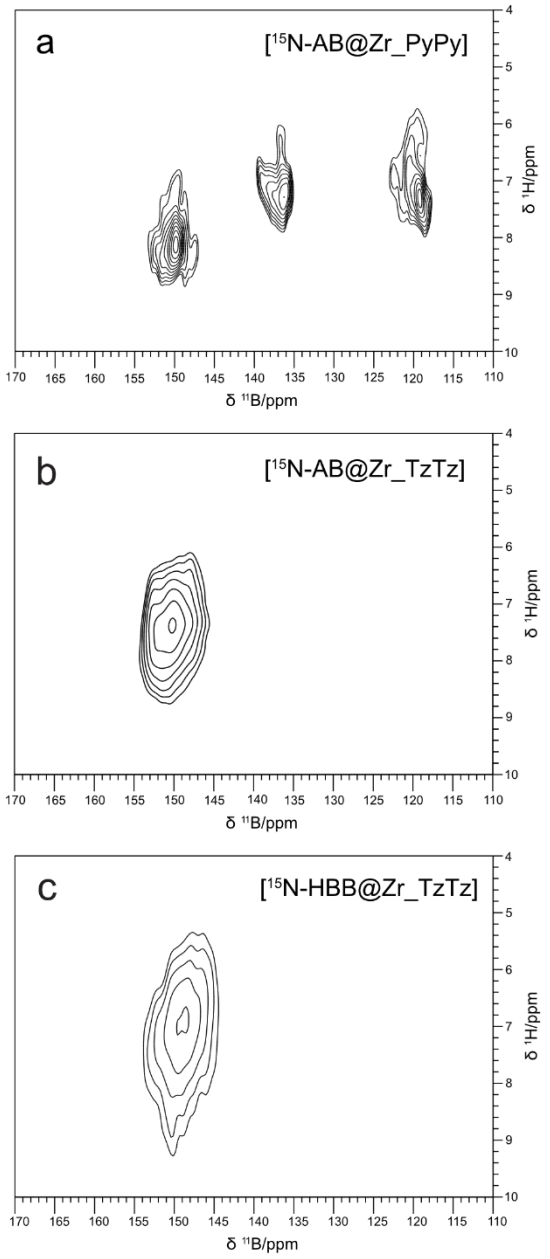

Figure S7. 2D ^{1}H-^{13}C FSLG HETCOR spectra of the loaded MOF: [^{15}N-AB@**Zr_PyPy**] (A), [^{15}N-AB@**Zr_TzTz**] (B), [HBB@**Zr_TzTz**] (C). The spectra were acquired with a 20.0 T (850 MHz of Larmor frequency), at a temperature of –8 °C and at 20 kHz of MAS frequency. The contact times were 100 μs. All the experimental and processing parameters are listed in Tables S3, S5, S7.

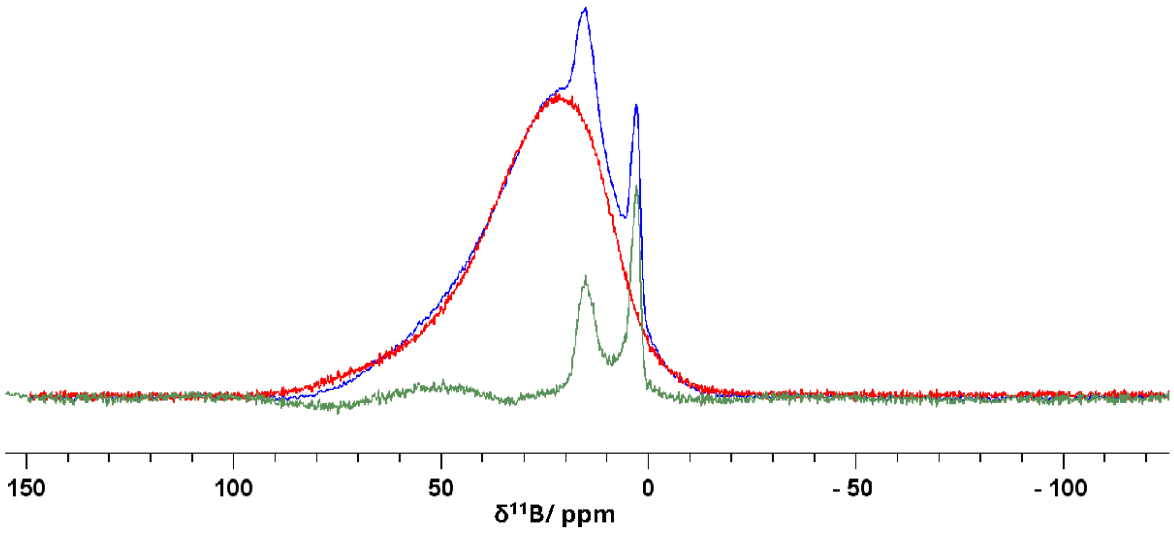

Figure S8. 1D ^{11}B Hahn echo spectra acquired on the loaded MOF [^{15}N-AB@**Zr_PyPy**] (blue line) and acquired with the same sequence and experimental conditions on the empty probe (red line), see Table S8 for the experimental and processing parameters. The broad bell-shaped resonance underlying the peaks corresponds to the probe background. The spectrum with subtracted background is drawn in green line. The distorted baseline in the region $40 \leq \delta_B \leq 100$ ppm is due to subtraction artifacts. The spectra were acquired at 16.4 T (700 MHz of proton Larmor frequency), using 4 mm rotors spinning at 12 kHz of MAS frequency and at a temperature of 25 °C. The ^{11}B spectra of the other loaded MOF samples were acquired with the same subtraction procedure.

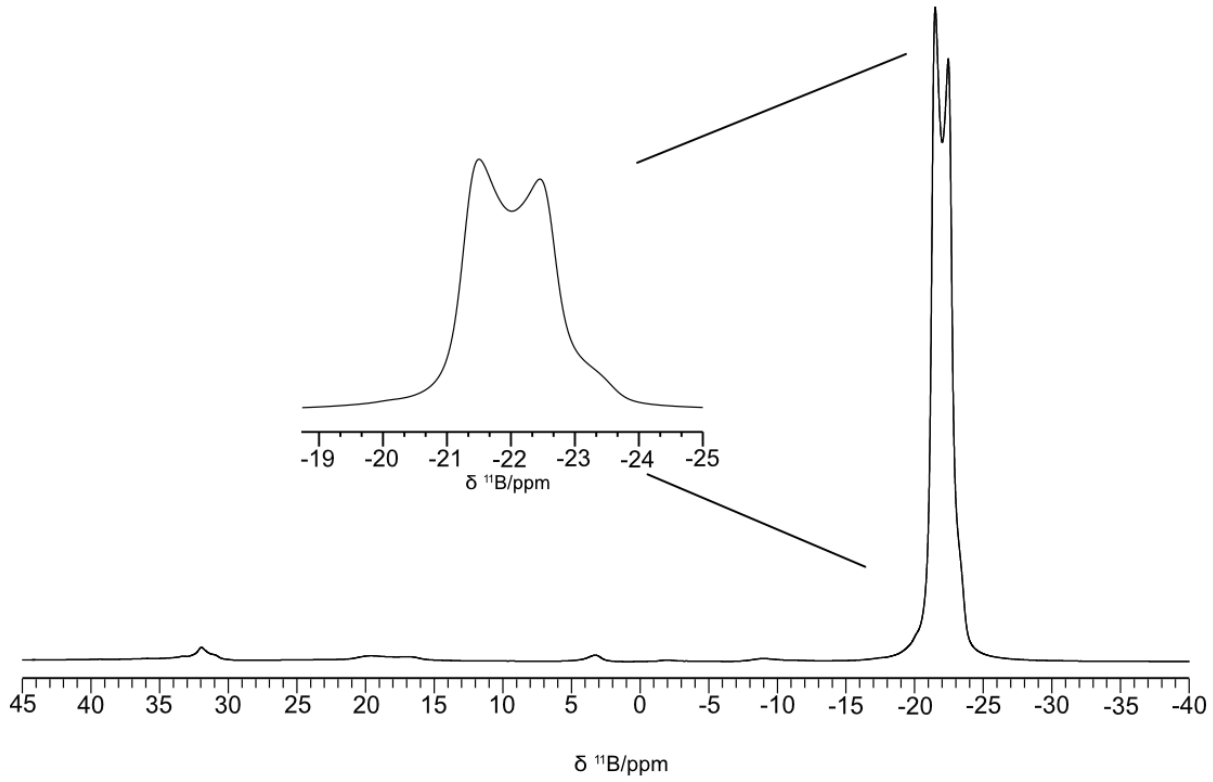

Figure S9. 1D ^{11}B Hahn echo spectra of pristine AB acquired at 16.4 T (700 MHz of proton Larmor frequency), using 4 mm rotors spinning at 12.0 kHz of MAS frequency and at a temperature of 25 °C. The inset shows an enlargement of the main peak at δ_B = –22 ppm showing the characteristic second order quadrupolar lineshape. The experimental and processing parameters are reported in Table S11.

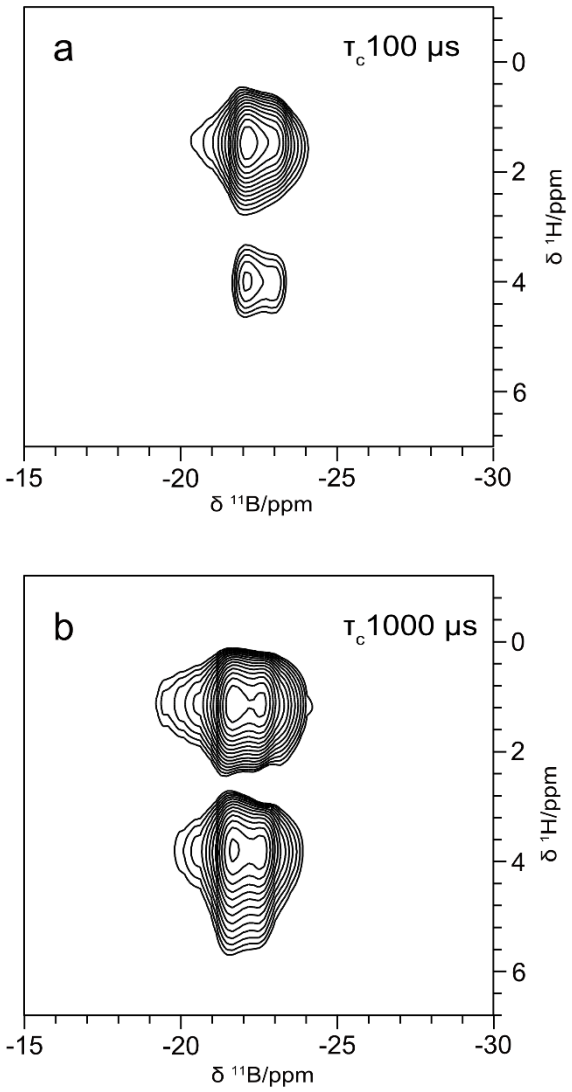

Figure S10. 2D ^{1}H-^{11}B 2D FSLG HETCOR spectra of pristine ^{15}N-AB (a), with a contact time of 100 μs where mainly the boron directly bonded protons are visible and (b) the same spectrum acquired with a contact time of 1000 μs, where ^{11}B atoms correlates with both the BH hydrogens (δ_H ≈1-2 ppm) and the NH hydrogens (δ_H ≈ 4-5 ppm). The spectra were acquired at 16.4 T (700 MHz of proton Larmor frequency) using 4 mm rotors spinning at 12.0 kHz of MAS frequency and at a temperature of 25 °C. The experimental and processing parameters are listed in Table S11.

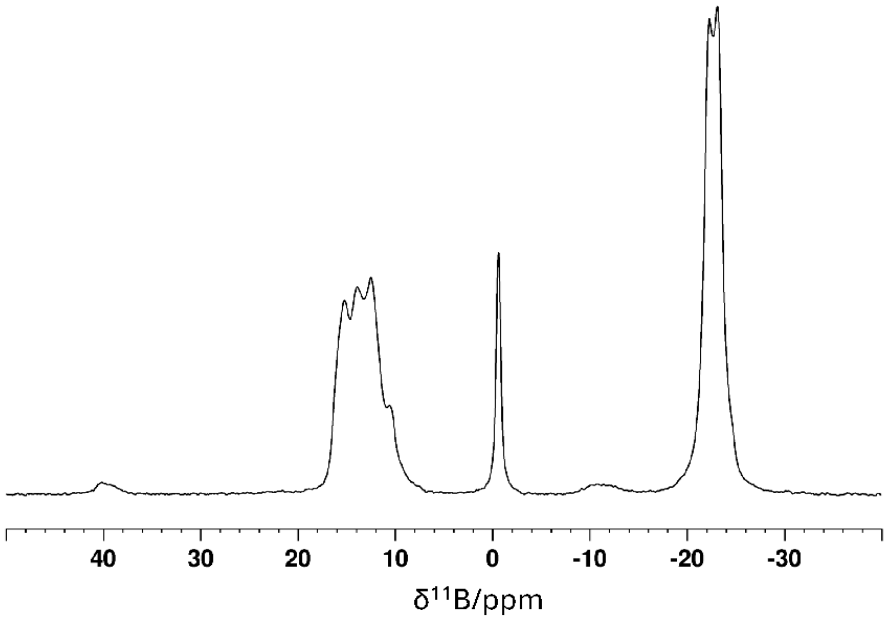

Figure S11. 1D ^{11}B Hahn-Echo spectra of HBB acquired at 16.4 T (700 MHz of proton Larmor frequency), using 4mm rotors spinning at 12 kHz of MAS frequency and at T = 25 °C. The resonances at $\delta_B \approx 0$ ppm and $\delta_B \approx 10$ ppm correspond to decomposition products; pure HBB has a single ^{11}B peak at $\delta_B = -22$ ppm showing the characteristic second order quadrupolar lineshape. Table S12 lists all the experimental and processing parameters.

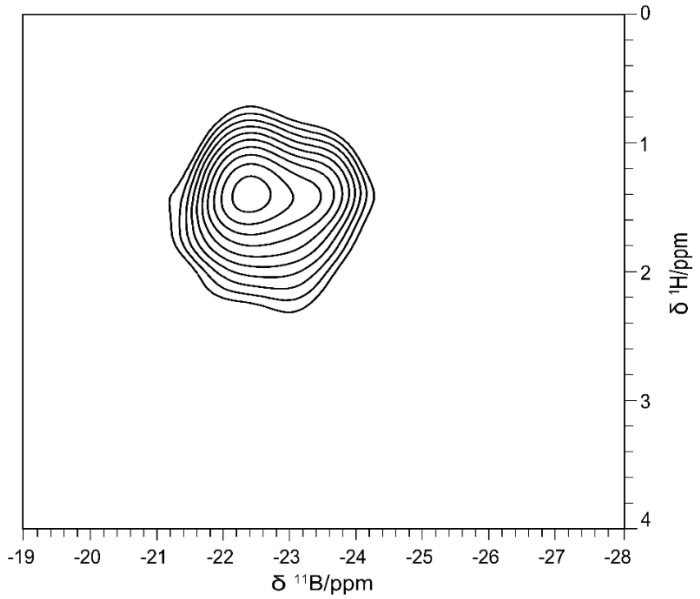

Figure S12. 2D ^{1}H-^{11}B 2D FSLG HETCOR spectra of HBB, with a contact time of 100 μs where mainly the boron directly bonded hydride protons are visible. The spectra were acquired at 16.4 T (700 MHz of proton Larmor frequency) using 4 mm rotors spinning at 12.0 kHz of MAS frequency and at a temperature of 25 °C. The experimental and processing parameters are listed in Table S12.

^{11}B NMR hydride quantification

In each spectrum, the signals were manually integrated used the software Bruker TOPSPIN (v. 4.1.4). The integral per scan of the ^{11}B peaks in each sample were compared to the integral per scan obtained on pure AB. The accurately weighted amount of sample was confined in the most sensitive part of the NMR rotor, in order to detect the signal of the entire portion of sample. On the bases of the relative integrals and the precise weighted amount we calculated the weight % of AB and HBB incorporated in the MOFs. The relative error of the integrated signals was estimated by the integral of the noise in different regions of the spectrum containing only noise.

Table S13. Experimental parameters used to quantify the amount of boron hydrides within the MOFs. The relative integrals were obtained with respect to those of boron in pure AB.

Sample	Weight (g)	Integral per scan relative to pure AB sample (10^{-3})	Hydride amount [wt.%]
^{15}N-AB@**Zr_PyPy**	0.0129 ± 0.0001	5.84 ± 0.06	0.593 ± 0.009
^{15}N-AB@**Zr_TzTz**	0.0337 ± 0.0001	35.0 ± 0.3	1.36 ± 0.01
^{15}N-HBB@**Zr_TzTz**	0.0231 ± 0.0001	2.8 ± 0.3	0.154 ± 0.017

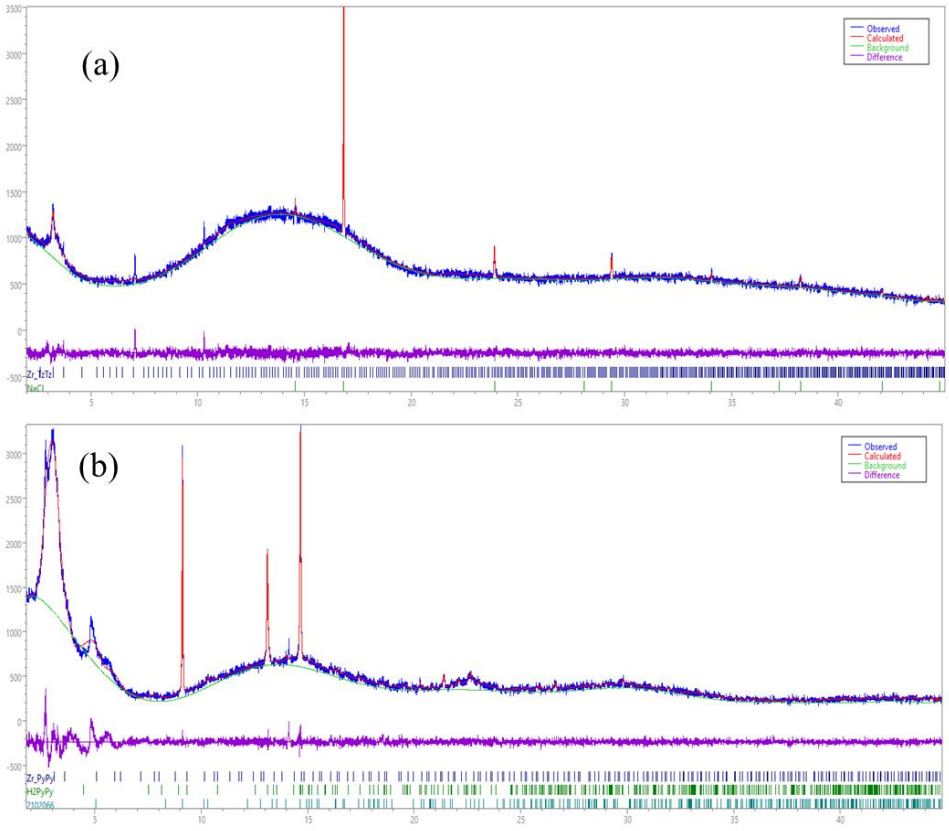

Figure S13. Rietveld fits of the high-resolution XRPD profiles of **Zr_TzTz** (a) and **Zr_PyPy** (b). NaCl impurity coming from the linker synthesis was found for the former, while some unreacted bipyridyl linker (**H_2PyPy**) was found in the latter.

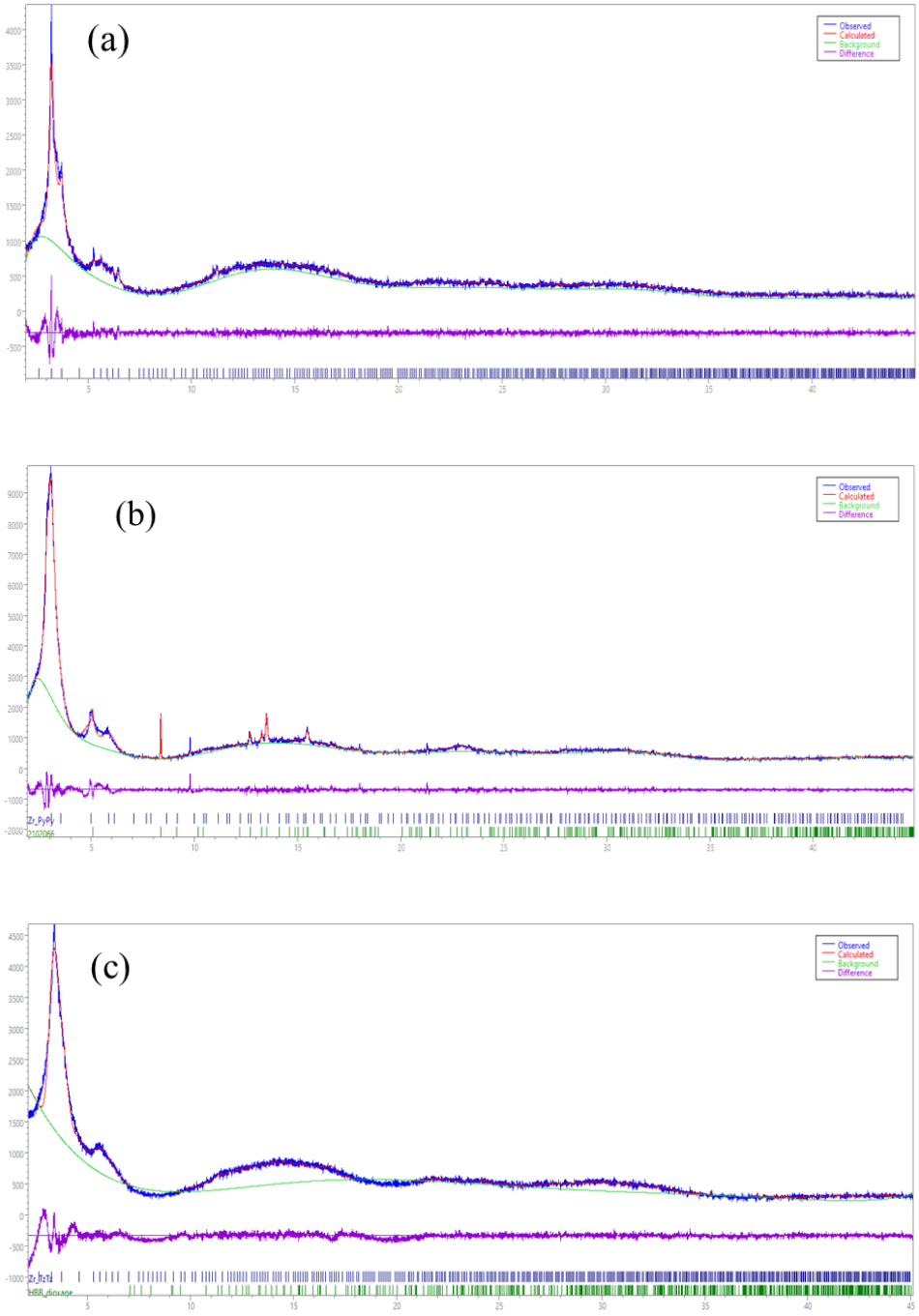

Figure S14. Rietveld fits of the high-resolution XRPD profiles of [AB@**Zr_TzTz**] (a) [AB@**Zr_PyPy**] (b) and [HBB@**Zr_TzTz**] (c). Some unreacted bipyridyl linker (**H_2PyPy**) was found in (b) as an impurity.

Table S14. Results of the Rietveld analysis on high-resolution XRPD profiles. Weighted agreement factor between observed and calculated profile (R_{wp}), crystal cell parameter.

Sample	R_{wp}	Crystal cell parameter (Å)
Zr_TzTz	4.2	25.33
Zr_PyPy	6.1	26.54
AB@**Zr_TzTz**	6.2	25.32
HBB@**Zr_TzTz**	12.6	25.32
AB@**Zr_PyPy**	5.6	26.50

PDF analysis on Zr_TzTz and Zr_PyPy.

A structural analysis of the empty MOFs has been carried out by using their structures present in the Cambridge Database as starting point. A direct comparison between observed and calculated PDF profiles (Figure S15a) highlights lacking of long-range order. Three sharp peaks characterize the observed profiles, which can be attributed to the metal center coordination, specifically to Zr-O (2.2 Å), Zr-Zr lateral (3.5 Å) and diagonal (4.9 Å) distances. Such peaks are expected to be repeated along the PDF profile after a distance corresponding to the organic linker, and in fact calculated profiles meet this expectation with a spacing of about 15 Å. Unfortunately, these second-order peaks are only hinted in the observed PDF profiles. It is worth noticing that the first-order peaks in the observed profiles are sharper with respect to the calculated ones. This suggests that the metal site is highly stable with respect to thermal motion (the actual Debye-Waller factors are much lower than those reported in the calculated models), and the rapid decrease in intensity at higher distances is due structural disorder. The fitting of the structural models is shown in Figure S15b, and fitted parameters are reported in Table S15. The rapid decrease of intensities has been

modelled by introducing a limited size of the crystalline domains, which have been estimated as 12 Å for **Zr_TzTz** and 21 Å for **Zr_PyPy**. The thermal motion of the metal centers is very limited, as expected, while those of the organic linker is about 1000 times greater.

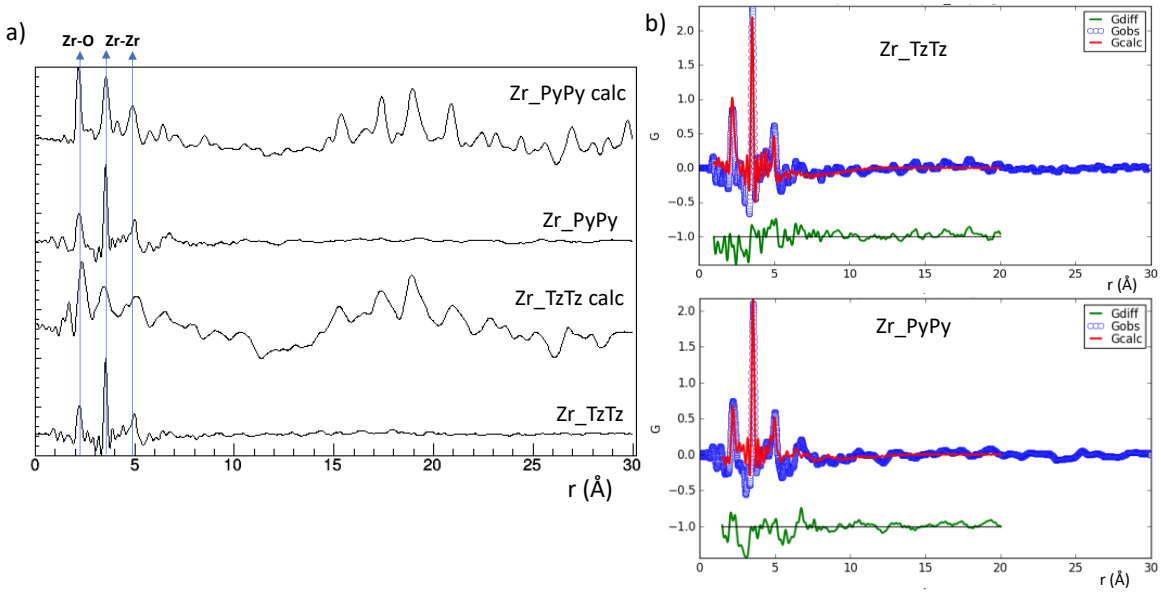

Figure S15. (a) Comparison of observed and calculated PDF profiles for **Zr_TzTz** and **Zr_PyPy**. The CIF files of **Zr_TzTz** (*Pn*$\bar{3}$, CCDC 1043281) and **Zr_PyPy** (*Fm*$\bar{3}$, CCDC 968930) have been used for calculations, where the crystal cell parameter has been set to the refined values shown in Table S15. The assignment of the three main peaks to Zr-Zr and Zr-O interatomic distances is highlighted with arrows. (b) Results of the PDF fit, where observed, calculated and difference profiles are shown in blue, red and green, respectively.

Table S15. Results of the structural refinement of PDF profiles. Reported parameters are: weighted agreement factor between observed and calculated profile (R_w), crystal cell parameter (*a*) and average size of the crystallites ($SP_{diamater}$), as estimated by the envelope of the PDF profile, thermal factor of Zr atoms (U_{Zr}) and of the remaining atoms ($U_{C,O,S}$).

	Zr_TzTz	**Zr_PyPy**
R_w	0.408	0.430
a (Å)	26.32	26.76
$SP_{diameter}$ (Å)	12.2	14.9
U_{Zr} (Å^2)	2×10^{-5}	7×10^{-6}
$U_{C,O,S}$ (Å^2)	0.01	0.01

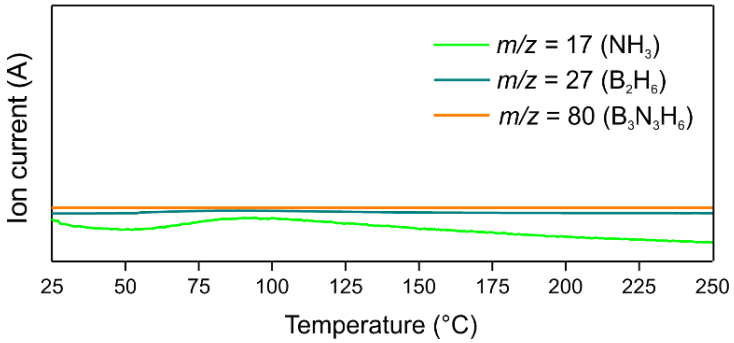

Figure S16. Mass survey of the main AB decomposition byproducts during the thermal treatment of [AB@**Zr_TzTz**].

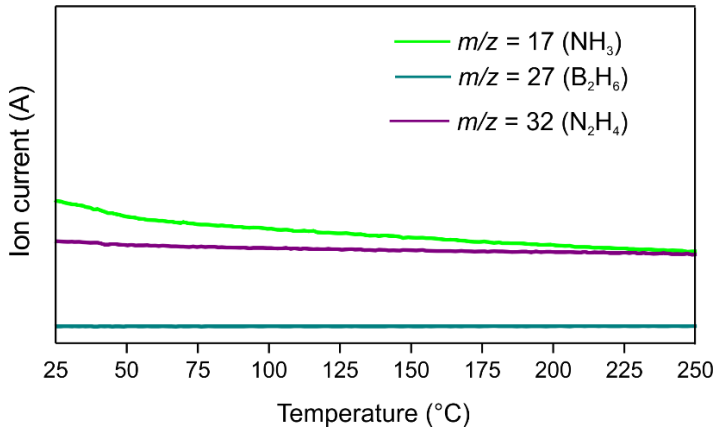

Figure S17. Mass survey of the main HBB decomposition byproducts during the thermal treatment of [HBB@**Zr_TzTz**].

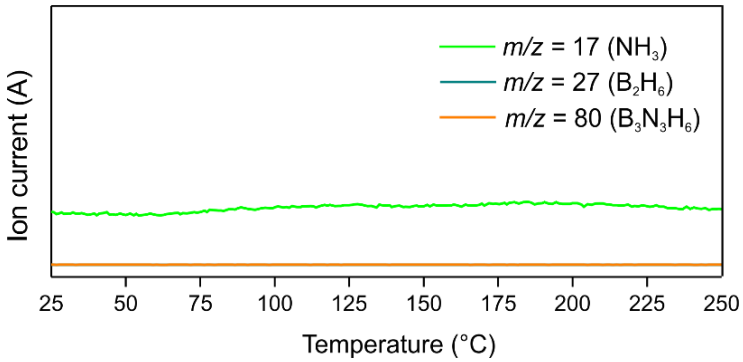

Figure S18. Mass survey of the main AB decomposition byproducts during the thermal treatment of [AB@**Zr_PyPy**].